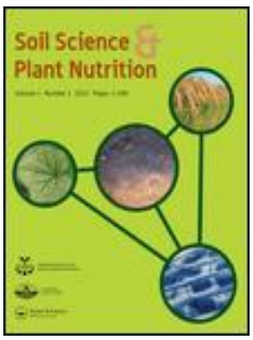

Soil Science and Plant Nutrition

ISSN: 0038-0768 (Print) 1747-0765 (Online) Journal homepage: http://www.tandfonline.com/loi/tssp20

Laboratory examination of greenhouse gaseous and microbial dynamics during thawing of frozen soil core collected from a black spruce forest in Interior Alaska

Hirohiko Nagano, Yongwon Kim, Bang-Yong Lee, Haruka Shigeta & Kazuyuki Inubushi

To cite this article: Hirohiko Nagano, Yongwon Kim, Bang-Yong Lee, Haruka Shigeta & Kazuyuki Inubushi (2018): Laboratory examination of greenhouse gaseous and microbial dynamics during thawing of frozen soil core collected from a black spruce forest in Interior Alaska, Soil Science and Plant Nutrition, DOI: 10.1080/00380768.2018.1525267

To link to this article: https://doi.org/10.1080/00380768.2018.1525267

Published online: 08 Oct 2018.

SOIL SCIENCE AND PLANT NUTRITION
https://doi.org/10.1080/00380768.2018.1525267

Laboratory examination of greenhouse gaseous and microbial dynamics during thawing of frozen soil core collected from a black spruce forest in Interior Alaska

Hirohiko Nagano [a,b], Yongwon Kim [c], Bang-Yong Lee[d], Haruka Shigeta[b] and Kazuyuki Inubushi[b]

[a]Nuclear Science and Engineering Center, Japan Atomic Energy Agency, Ibaraki, Japan; [b]Graduate School of Horticulture, Chiba University, Matsudo, Japan; [c]International Arctic Research Center, University of Alaska Fairbanks, Fairbanks, AK, USA; [d]Division of Polar Climate Sciences, Korea Polar Research Institute, Incheon, Korea

ABSTRACT

In this study, we conducted an incubation experiment on a frozen soil core collected from a black spruce forest in Interior Alaska, in order to investigate potential changes in greenhouse gaseous (GHG) and microbial dynamics during thawing of frozen soil. The soil thawing is an important environmental process determining the annual GHG balance in the northern high-latitude ecosystem. A core spanning the ground surface to upper permafrost with a depth of 90 cm was vertically grouped into three layers (top, middle, and bottom layers). Then, 12 soil samples from 3 layers (i.e., 4 soil samples per layer) were incubated for 3 weeks, and net carbon dioxide (CO_2) and methane (CH_4) release/uptake rates were estimated. During the incubation, temperature was changed weekly from 0 to 5, then 10°C. The net amounts of CO_2 released by six of the eight soil samples from the top and middle layers were 1.5–19.2-fold greater at 5°C than at 0°C, while the release at 10°C was reduced in the cases of three of these six soil samples. Net CH_4 release was the greatest in bottom-layer soil samples incubated at 0°C. Then, low but apparent CH_4 release was observed in top and middle-layer soil samples incubated at 0°C. At 5 and 10°C, net CH_4 release from bottom-layer soil samples was decreased. Then, net CH_4 uptake was observed in the top and the middle-layer soil samples. Both net uptake and release of CH_4 were reduced upon the addition of a chemical inhibitor (i.e., 2-bromoethane sulfonate) of anaerobic methanotrophic and methanogenic activity. The bacterial and archaeal community structures based on 16S rRNA amplicon analysis were changed along the depth, while they were less changed during thawing. Thus, it was found that soil GHG dynamics responded sensitively and variously to thawing, while there was less change in 16S rRNA-based microbial community structures during the thawing progress.

ARTICLE HISTORY
Received 23 April 2018
Accepted 14 September 2018

KEYWORDS
Black spruce forest; greenhouse gas; next-generation sequencing; permafrost; soil thaw

1. Introduction

During the onset of the spring season (i.e., the thawing season) in northern high-latitude ecosystems underlain with permafrost and a seasonally frozen active layer, many researchers (e.g., Friborg *et al*. 1997; Kim *et al*. 2007, 2012; Tokida *et al*. 2007) have observed episodic release of methane (CH_4), a greenhouse gas (GHG) with the second largest contribution to the global warming behind carbon dioxide (CO_2) (IPCC 2013). Such episodic CH_4 release can contribute significantly to the annual CH_4 budgets of these ecosystems (Friborg *et al*. 1997). The major origin of episodic release of CH_4 is the CH_4 trapped in the frozen active layer soils and permafrost (Friborg *et al*. 1997; Kim *et al*. 2007).

Soil thawing affects soil microbial processes associated with GHG production and consumption (Kim *et al*. 2012). The thawing of frozen soil enhances various soil environmental conditions, such as substrate availability, temperature, moisture, and aeration (Kim *et al*. 2012). These changes, in turn, directly affect microbial activity (Chen *et al*. 2003; Kim *et al*. 2012). In general, as thawing progresses, soil organic matter decomposition (i.e., CO_2 production) and CH_4 oxidation are expected to occur in the upper aerobic layer, while CH_4 production is to occur in the deeper anaerobic layer. Consequently, whether a northern ecosystem soil becomes a GHG sink or a source during thawing depends on the microbial activity along the soil profile.

Byun *et al*. (2017) recently found a sharp increase in CH_4 concentration (from 1 to 200 μmol L^{-1}) along the depth of a frozen soil core collected from a poorly drained black spruce (*Pinus mariana*) forest in Interior Alaska. The CH_4 entrapped in deep frozen soils was likely produced by anaerobic microbial processes during or before the soils froze (Byun *et al*. 2017). Then, the vertical profile of the bacterial and archaeal communities in this soil core was investigated by Tripathi *et al*. (2018). However, the response of frozen soils in this forest to thawing was not investigated. Mackelprang *et al*. (2011) observed rapid changes in the carbon and nitrogen cycling, as well as various microbial gene abundances, in response to soil thawing in another Alaskan forest.

In this study, we conducted an incubation experiment involving thawing a frozen soil core (ground surface to upper permafrost; 90 cm long) collected from the black spruce forest investigated by Byun *et al*. (2017) and Tripathi *et al*. (2018). During incubation, we compared the changes in net CO_2 and CH_4 release/uptake rate at three depths (top, middle, and bottom layers) and thawing progress (0, 5, and 10°C). Then, we analyzed the genomic information of the bacterial and archaeal community

CONTACT Hirohiko Nagano nagano.hirohiko@jaea.go.jp Nuclear Science and Engineering Center, Japan Atomic Energy Agency, Tokai, Naka, Ibaraki 319-1195, Japan

structures in the soil by using the next-generation sequencing (NGS) technique for 16S rRNA amplicons (Caporaso *et al*. 2012; Klindworth *et al*. 2013) to examine the changes in soil microbial community structures during the thawing progress.

2. Materials and methods

2.1. Study site

The study site was the JICS (JAMSTEC-IARC Collaboration Study) supersite (65°07′24″ N, 147°29′15″ W) in a black spruce forest underlain by discontinuous permafrost within the property of the Poker Flat Research Range of University of Alaska Fairbanks. The landscape of this forest comprises a large fraction of understory vegetation, such as mosses (*Sphagnum fuscum* and *Hylocomium splendens*), shrubs (*Ledum groenlandicum, Vaccinium uliginosum, Rubus chamaemorus, Betula glandulosa*, and *Betula nana*), sedges (*Eriophorum vaginatum*), and lichen (*Cladina stellaris*) (Ikawa *et al*. 2015). The JICS supersite is an Ameriflux site (registered as US-Prr) established in 2009 with the eddy covariance system for year-round CO_2 and water exchange observation (Ikawa *et al*. 2015; Nakai *et al*. 2013; Nagano *et al*. 2018) to understand carbon and hydrological cycling in boreal forest ecosystems (e.g., Byun *et al*. 2017; Kobayashi *et al*. 2016; Miyazaki *et al*. 2015; Nagai *et al*. 2013; Sueyoshi *et al*. 2015; Sugiura *et al*. 2011; Suzuki *et al*. 2015).

2.2. Soil core sampling

On 3 May 2013, a frozen soil core was collected at a sphagnum moss regime underlain by discontinuous permafrost within the JICS supersite (Byun *et al*. 2017). The soil core used in this study was collected from a point adjacent to the sampling point in Byun *et al*. (2017). After the removing of snow covering the frozen ground, a SIPRE coring auger (76.2 mm diameter, 90 cm length; Jon's Machine Shop, Fairbanks, AK, USA) with an inner polyvinyl chloride liner (S-11362, 75 mm in diameter, 900 mm in long, Uline, Seattle, WA, USA) was drilled into the ground down to the upper permafrost layer at a depth of 90 cm. In our soil core, the top of permafrost layer was found around 70–80 cm depth. Then, the auger was retrieved with soil core sample. The collected soil core was maintained under freezing conditions both during the transport to Japan and until its use in the experiments.

2.3. Preparation of soil samples

The frozen soil core was vertically grouped into three layers (top, middle, and bottom layers), with each layer measuring 30 cm in depth. Then, the longitudinal core was cut into 32 subsamples at intervals of 2–3 cm along the depth. Four subsamples per layer (Table 1) were incubated. The other subsamples were stored at −20°C for future use. The incubated subsamples were individually broken into small pieces and placed in sterilized glass bottles (100 mL volume, Nichiden-Rika Glass, Osaka, Japan). Bottles containing the soil subsamples (2–15 g fresh weight equivalent to 0.2–5.5 g dry weight) were sealed with sterilized butyl stoppers and flushed with sterilized air + 10 ppm CH_4 (top-layer soil subsamples) or nitrogen gas (N_2) + 10 ppm CH_4 (middle and bottom-layer soil subsamples). Six bottles per subsample were prepared for incubation. All works during the preparation were conducted on ice to keep the samples frozen.

2.4. Soil incubation

Soil samples were incubated for 3 weeks, and the incubation temperature was changed weekly from 0 to 10°C in steps of 5°C. This temperature change rate is similar warming rate in the field, where changes in surface soil temperature (0–10°C) are frequently observed for a month after the start of thawing. Immediately before the start of incubation, 1 mL of 210 mM 2-bromoethane sulfonate (BES) solution was added to one of the six bottles. BES is a well-known inhibitor of anaerobic microbial CH_4 oxidation and production (Mackelprang *et al*. 2011). The incubation of all bottles was initiated at 0°C. A week later, ca. 30 mL of gas was collected from each bottle into vacuumed glass vials (20 mL volume) for measuring net CO_2 and CH_4 release/uptake rates. Then, the bottle with BES and one of the five bottles without BES were removed from the incubator and stored at −20°C until they were used for analyzing microbial DNA, soil carbon, soil nitrogen, and soil moisture. After the flushing of air + 10 ppm CH_4 (for top-layer soils) or N_2 + 10 ppm CH_4 (for middle and bottom-layer soils) in all remaining bottles and the addition of 1 mL BES solution to the one remaining bottles, these bottles were incubated at 5°C. A week later, gas collection, bottle removal, gas flushing, and BES addition were conducted in the same manner as that at the end of the incubation at 0°C. After incubation at 10°C for a

Table 1. Description[†] of soil subsamples used in incubation experiment involving thawing of frozen soil core (down to 90 cm depth) collected from a black spruce forest in Interior Alaska.

Layer	Subsample ID	Range of depth (cm)	Water content (g water g^{-1} dry soil)	Total carbon (C) (mg g^{-1} dry soil)	Total nitrogen (N) ([mg g^{-1} dry soil)	C/N ratio
Top	1	5–10	12.1 ± 1.5	445 ± 11	4.3 ± 0.6	105 ± 12
	2	11–15	16.9 ± 1.8	429 ± 29	24.9 ± 0.5	17 ± 1
	3	16–20	16.3 ± 1.9	111 ± 3	11.5 ± 0.0	10 ± 0
	4	21–25	9.1 ± 1.1	429 ± 16	9.1 ± 0.2	47 ± 2
Middle	5	36–40	4.2 ± 0.5	436 ± 10	18.5 ± 1.9	24 ± 3
	6	41–45	3.5 ± 0.2	476 ± 27	32.9 ± 11.4	16 ± 8
	7	46–50	2.3 ± 1.1	413 ± 26	36.7 ± 1.4	11 ± 0
	8	51–55	2.6 ± 1.6	28 ± 6	1.3 ± 0.2	21 ± 2
Bottom	9	66–70	6.2 ± 1.5	73 ± 54	16.9 ± 5.7	4 ± 2
	10	71–75	6.2 ± 0.9	75 ± 16	1.2 ± 0.4	65 ± 8
	11	76–80	1.0 ± 0.2	60 ± 4	1.0 ± 0.1	59 ± 10
	12	81–85	0.6 ± 0.1	96 ± 5	19.8 ± 0.4	5 ± 0

[†]Water content, total carbon, total nitrogen, and carbon/nitrogen ratio are presented as mean ± standard deviation (n = 3).

week, the gases in the bottles were collected, and these bottles were stored with the other bottles stored previously until the analyses.

2.5. Net GHG release/uptake rate measurement

In this study, net GHG release/uptake rate is presented as the weekly rate of change in GHG concentration per gram of dry soil (i.e., ppm or % g^{-1} dry soil $week^{-1}$). GHG concentration in the gas samples collected for incubation was determined using a gas chromatograph (GC-14B, Shimadzu, Kyoto, Japan) equipped with a thermal conductivity detector for CO_2 or a frame-ionized detector for CH_4. Then, the release/uptake rate was calculated by comparing GHG concentrations between the collected gas samples and the flushed gases (air + 10 ppm CH_4 or N_2 + 10 ppm CH_4). Owing to procedural limitations of the incubation experiment, in this study, net release/uptake rate data of each subsample without BES addition were presented as mean values calculated from five (incubation at 0°C) or three (incubation at 5°C) repetitions, or as the value from a single repetition (incubation at 10°C).

2.6. Microbial DNA analysis

Bacterial and archaeal community structures in soils incubated without BES were analyzed using the NGS technique (Caporaso *et al*. 2012; Klindworth *et al*. 2013) and an Illumina MiSeq System (Illumina, CA, USA) for 16S rRNA amplicons. Total genomic DNA in soils (0.5 g fresh weight) was extracted using the FastDNA SPIN Kit for Soil (MP Biomedicals, CA, USA) and purified with PowerClean DNA Clean-Up Kit (Mo Bio Laboratories, CA, USA). Then, total genomic DNA samples from the top- and the middle-layer soils were sent to TaKaRa Bio (Shiga, Japan) for sequencing analysis. The bottom layer was not subjected to sequencing analysis because the amounts of DNA extracted from the bottom-layer soils were thought to be insufficient for sequencing, based on the results of agarose gel electrophoresis after DNA extraction. Amplification of the V3–V4 region of the 16S rRNA genes in the samples was conducted using the 16S (V3–V4) Metagenomic Library Construction Kit for NGS (TaKaRa Bio) coupling with the Nextera XT Index Kit (Illumina). Then, the amplicons purified with AMPureXP (Beckman Coulter, CA, USA) were sequenced with a MiSeq (Illumina) by using a MiSeq Reagent Kit v3 (Illumina) for generating 2 × 250 bp paired end reads. A total of 11.4 million reads with 2.9 Gb (>90% of bases had quality score higher than 30, equivalent to a 0.001 error rate) were obtained from 24 total genomic DNA samples (2 layers × 4 subsamples × 3 temperature levels). The obtained forward and reverse reads were ensembled to 2.3 million pair-end sequences, and these sequences were then binned into 1325 operational taxonomic units (OTUs) by using CD-HIT-OUT (Li *et al*. 2012) configured with a clustering threshold value of 0.97 and per-base PCR error value of 0.01. The Illumina datasets obtained in this study are available at NCBI (National Center for Biotechnology Information) GenBank with the accession numbers from SRR7012866 to SRR7012889.

Taxonomies of the OTUs were determined using Quantitative Insights Into Microbial Ecoclogy (QIIME; Caporaso *et al*. 2012), an open-source software pipeline for analysis of microbial community sequence data. In the QIIME analysis, OTU sequences were classified with the RDP classifier (Wang *et al*. 2007) by using a 16S rRNA gene database, GreenGenes (gg_13_18 ver.; DeSantis *et al*. 2006). Finally, relative abundances of a total of 32 phyla (30 for bacteria, 2 for archaea) were obtained from the 1325 OTUs.

2.7. Soil water, carbon, and nitrogen contents

Portions of soils incubated without BES were used for the measurement of water, carbon, and nitrogen contents in soil (Table 1). Soil water contents were determined from differences in soil weight before and after overnight drying at 100°C. Then, carbon and nitrogen contents in soil samples were measured using a carbon nitrogen analyzer (MT500, Yanaco New Science, Kyoto, Japan). Because of the limited amounts of soil samples, the samples dried after the measurement of the water content were used for the analyses of carbon and nitrogen contents.

2.8. Statistical comparison

Statistical comparisons for examining significant effects of temperature, soil sampling depth, and their interaction on net GHG release/uptake rate and microbial community structure were performed with R software ver. 3.2 (R Core Team 2017). The two-way ANOVA test was applied for the comparison of net GHG release/uptake rate data. The comparisons of net GHG release/uptake rate were conducted separately for individual layer because the scales of values were largely different among three layers. Then, net GHG release/uptake rate data were normalized separately for individual depth with average and standard deviation of the depth of interest, in order to remove the effect of different scaling of values among depths. These normalized data for all depths were compared to examining significant differences in changing patterns of GHG release/uptake among all sample depths. The comparison of 16S rRNA-based microbial community structures among different soil sample depths and incubation temperatures was conducted with the permutational multivariate analysis of variance (perMANOVA, 9999 random permutations) by *adonis* function in *vegan* package (Oksanen *et al*. 2018). In the comparison by perMANOVA, read frequencies of OTUs representing microbial community structures were converted to pairwise Bray–Curtis dissimilarity matrices. Then, nonmetric multidimensional scaling (NMDS) technique was applied for visualizing the pairwise Bray–Curtis dissimilarity matrices in two-dimensional plotting. NMDS was performed with *metaMDS* function in *vegan* package (Oksanen *et al*. 2018).

3. Results

3.1. Net GHG release/uptake rate

Net CO_2 release was greater at 5°C than at 0°C in most soil samples of top (0–30 cm depth) and middle (30–60 cm depth) layers, while net CO_2 release at 10°C was reduced in a few top- and middle-layer soils (Fig. 1). In six of the eight soil samples

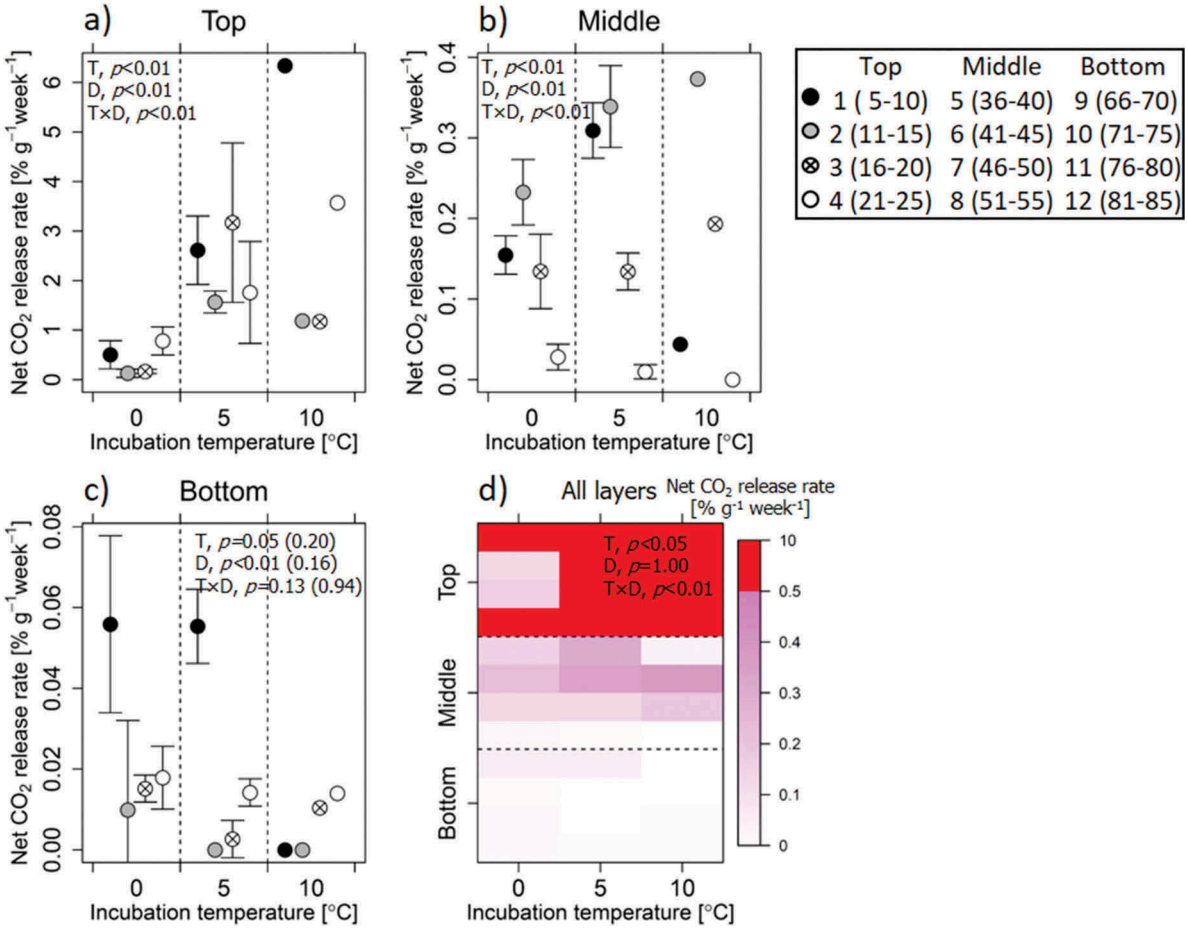

Figure 1. Net carbon dioxide (CO_2) release rates from soil core samples incubated under weekly changing temperatures from 0 to 10°C in intervals of 5°C, without the addition of 2-BES, a chemical inhibitor for anaerobic methane oxidation and production (n = 5 at 0°C, n = 3 at 5°C, and n = 1 at 10°C). Top and bottom-left panels (a–c) show the release rate separately for the individual soil layer (i.e., top, middle, or bottom layer). Bottom-right panel (d) represents the release rate through the all soil sample depths. Significant p levels for effects of temperature (T), soil sample depths (D), and their interaction ($T \times D$) were determined by two-way ANOVA test, then they are presented on top-left side (a and b) or top-right side (c and d) of panels. Two-way ANOVA test for the release rate through the all soil sample depths was applied for the release rate normalized for individual depth (see the main text for details).

from the top and middle layers, net CO_2 release at 5°C (0.31–3.17% g^{-1} dry soil day^{-1}) was 1.5–19.2-fold greater than that at 0°C. Then, in three of these six soil samples, net CO_2 release at 10°C (0.4–6.3% g^{-1} dry soil day^{-1}) was 1.1–2.4-fold greater than that at 5°C, while net CO_2 release from other three soil samples at 10°C (0.04–1.17% g^{-1} dry soil day^{-1}) decreased to 14–76% of that at 5°C. Net CO_2 release from the bottom-layer soil samples (60–90 cm) (<0.06% g^{-1} dry soil day^{-1}) was less than 21% of the mean CO_2 release from the top and middle layers (0.21% g^{-1} dry soil day^{-1}).

The interactions between incubation temperatures and soil depths for top- and middle-layer soil samples were statistically significant at $p < 0.01$ with apparent single effect from each factor at $p < 0.01$ (Fig. 1). Then, there was less significance ($p = 0.13$) of the temperature–depth interaction for the bottom layer samples. The removal of data for most upper soil samples of the bottom layer resulted to less significance of single effects individually from temperatures ($p = 0.20$) and depths ($p = 0.16$). The interactions between temperatures and depths were statistically significant ($p < 0.01$) even after the normalization of net CO_2 release rate within individual depth, together with significant single effect of temperature at $p < 0.05$.

Net CH_4 release was observed in the soil samples of all three layers incubated at 0°C, while net CH_4 uptake was apparent in the top- and middle-layer soil samples that were incubated at warmer temperatures (Fig. 2). The greatest CH_4 release (51–105 ppm g^{-1} dry soil $week^{-1}$) was observed during incubation of the bottom-layer soil samples at 0°C. CH_4 was released at the rate of 1–13 ppm g^{-1} dry soil $week^{-1}$ from the top- and middle-layer soil samples during incubation at 0°C. After the temperature was raised to 5°C and then to 10°C, net CH_4 uptake (1–17 ppm g^{-1} dry soil $week^{-1}$) was observed in the top- and upper-middle soil samples. CH_4 was released from the lower-middle- and bottom-layer soil samples even after the temperature was increased to 5°C and then to 10°C, while the rate of release (1–16 ppm g^{-1} dry soil $week^{-1}$) was lower than that during the incubation at 0°C.

The interactions between incubation temperatures and soil depths were statistically significant for top and bottom layer soil samples at $p < 0.01$, with apparent single effect from each factor at $p < 0.01$ (Fig. 2). For middle-layer soil samples, single effect of soil depth was statistically significant at $p < 0.01$. Statistically significant ($p < 0.01$) effect of temperature was found even after the normalization of net CH_4 release/uptake rate within individual depth.

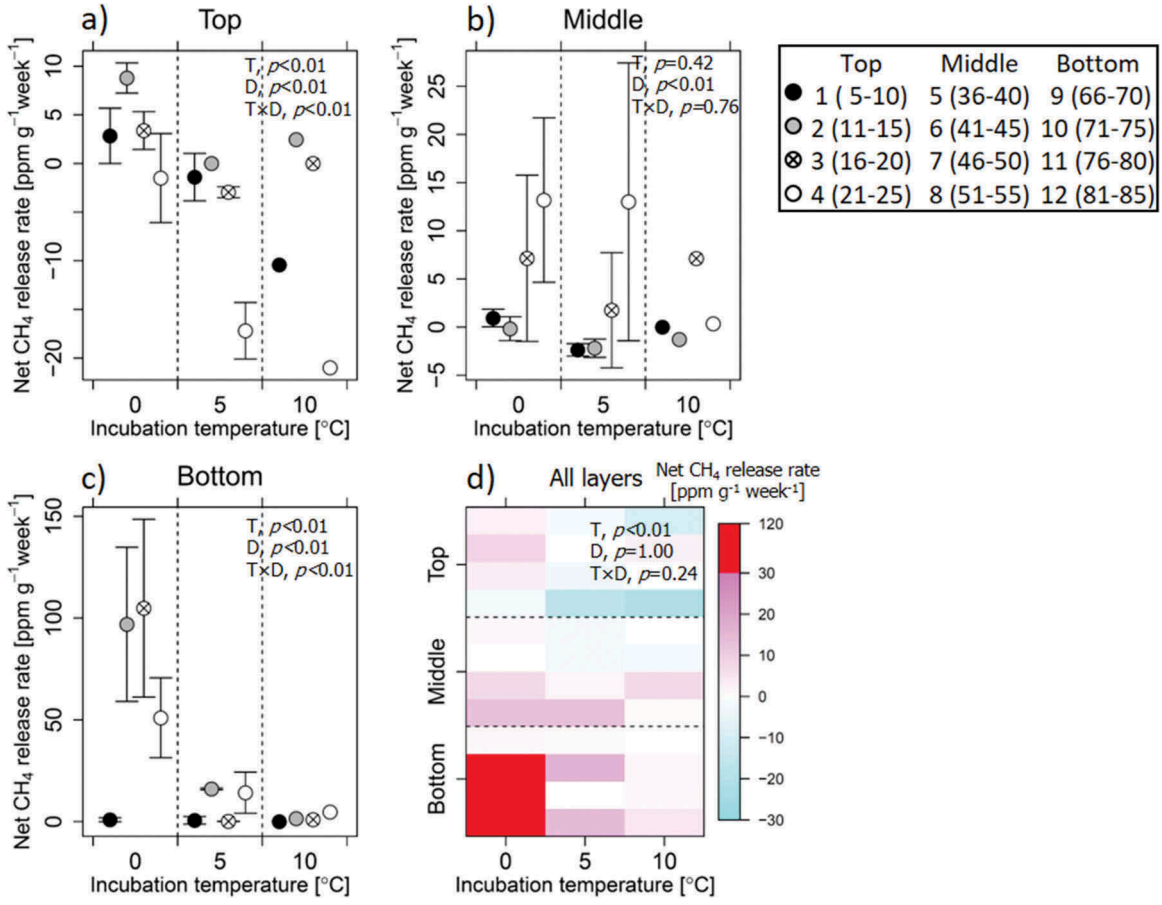

Figure 2. Net methane (CH_4) release/uptake rates from soil core samples incubated under weekly changing temperatures from 0 to 10°C in intervals of 5°C, without the addition of BES (n = 5 at 0°C, n = 3 at 5°C, and n = 1 at 10°C). Top and bottom-left panels (a–c) show the release rate separately for the individual soil layer (i.e., top, middle, or bottom layer). Bottom-right panel (d) represents the release rate through the all soil sample depths. Net CH_4 release rates are presented in positive values, then the uptake rates are in negative values. As in the same manner with the CO_2 release rate, significant p levels for effects of temperature (T), soil sample depths (D), and their interaction ($T \times D$) by two-way ANOVA test are presented on top-right side of panels.

The effect of BES on net CH_4 release/uptake varied depending on temperature (Fig. 3). Net CH_4 release at 0°C during the incubation with BES (1–116 ppm g^{-1} dry soil $week^{-1}$) was similar to that during the incubation without BES (1–105 ppm g^{-1} dry soil $week^{-1}$). However, at 5 and 10°C, net CH_4 release during the incubation without BES (0–16 ppm g^{-1} dry soil $week^{-1}$) decreased to 0–3 ppm g^{-1} dry soil $week^{-1}$ during the incubation with BES. Net CH_4 uptake (1–21 ppm g^{-1} dry soil $week^{-1}$ during the incubation without BES) decreased to 0 ppm g^{-1} dry soil $week^{-1}$ (four samples of top- and middle-layer soils at 5°C and a middle-layer soil sample at 10°C) or to 2–9 ppm g^{-1} dry soil $week^{-1}$ (one top-layer soil sample at 5°C and two top-layer soil samples at 0°C) upon the addition of BES.

3.2. 16S rRNA-based microbial community structures

16S rRNA-based microbial community structures were changed along the depth from the top to the middle layers, but they were less changed during thawing progress (Fig. 4). Regardless of the temperature, *Proteobacteria* was the most abundant phylum (25–37%; hereinafter, percentage value represents the relative abundance of phylum) in the top-layer soil samples, while the most abundant phylum in the middle-layer soil samples was *Actinobacteria* (24–37%) or *Acidobacteria* (10–41%). The relative abundance of *Proteobacteria* in the middle-layer soil samples was 13–24%. Then, the abundance of *Cyanobacteria*, the fourth most dominant phylum in most surface soil samples of the top layer (7–15%), decreased gradually as the depth increased (<1% in the deepest soils of the top layer). In contrast to *Cyanobacteria*, the relative abundances of AD3 and *Chloroflexi* increased gradually from <3% in the top-layer soil samples to >15% in the middle-layer soil samples. Apparent changes in relative abundance with increasing temperature were found only for *Firmicutes* in the upper two soil samples of the middle-layer (<1% at 0°C, and up to 12% at 10°C).

Changes in both community structures of archaea and bacterial methanotrophs along the depth were also observed in the middle-layer soil samples (Fig. 5). In the middle-layer soil samples, relative abundances of archaea to the overall community increased as the depth increased (from <0.1% in the upper middle-layer soil samples to 0.6% in the deeper middle-layer soil samples). Then, the dominant archaea changed from *MBGA* (a class of Crenarchaeota) in the upper middle-layer soil samples to *Methanomicrobia* (a class of Euryarchaeota) in the deepest

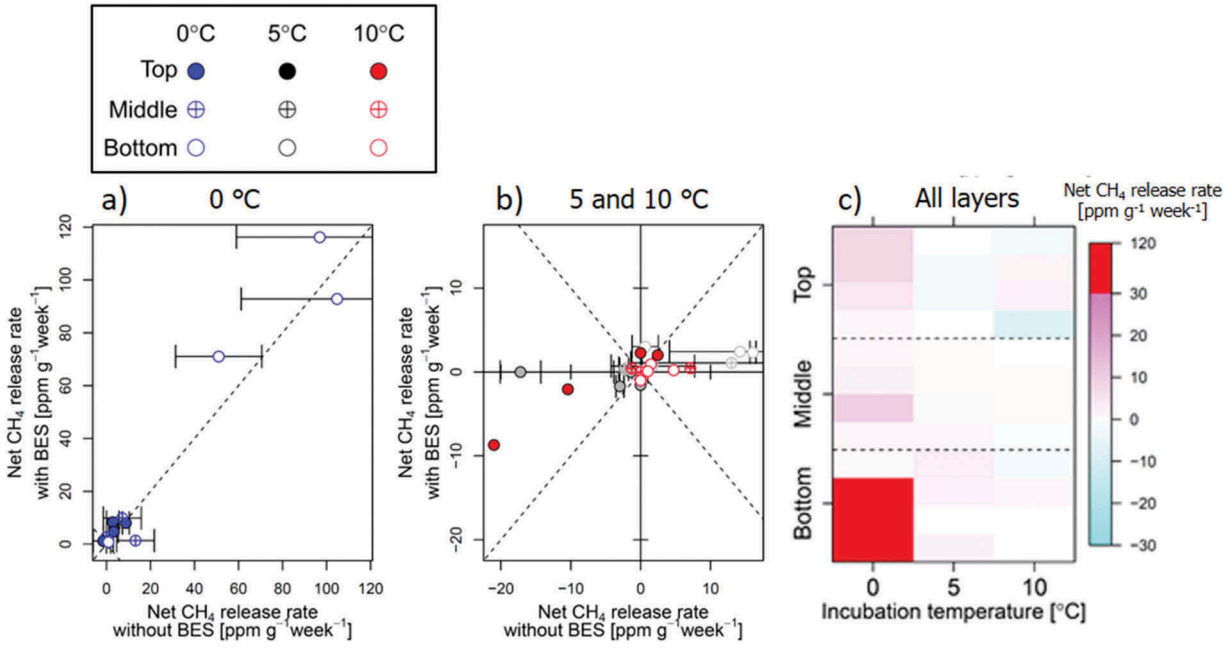

Figure 3. Comparison of net CH_4 release/uptake rates between incubations with/without BES addition. Left top panel represents for 0°C, then right top panel is for 5 and 10°C. Bottom left panel shows net CH_4 release/uptake rates for the incubation with BES through the all soil sample depths (n = 1).

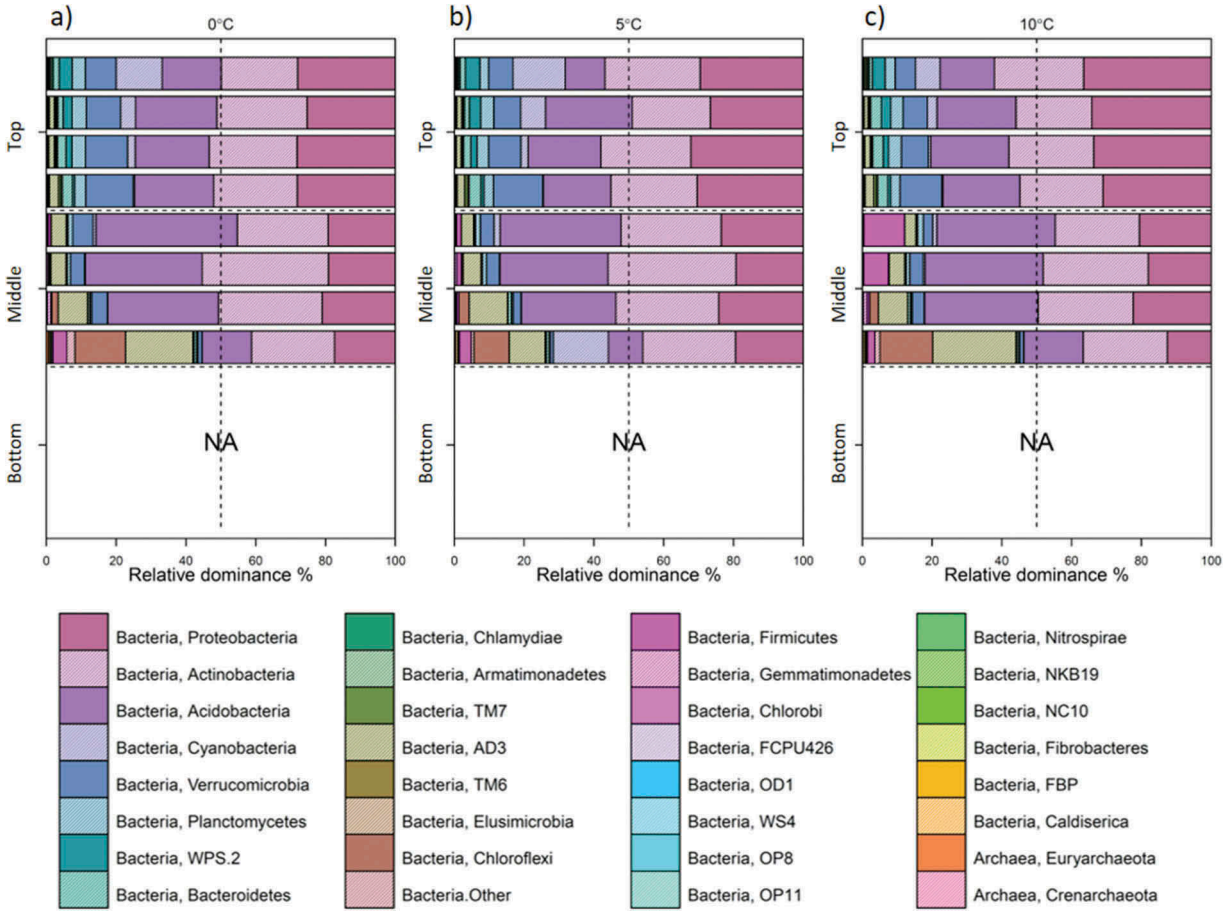

Figure 4. Relative abundances of bacterial and archaeal phyla in soil core samples incubated under weekly changing temperatures from 0°C (a) to 5°C (b), then 10°C (c), without the addition of BES. Presented data are obtained from an analysis conducted using a next-generation DNA sequencer (MiSeq, Illumina, Inc., CA, USA) for 16S rRNA amplicons of metagenomic DNA extracted from incubated soils. Detailed information about DNA analysis are presented in the main text. Data on bottom-layer soils are not available (NA) because of insufficient amounts of extracted DNA.

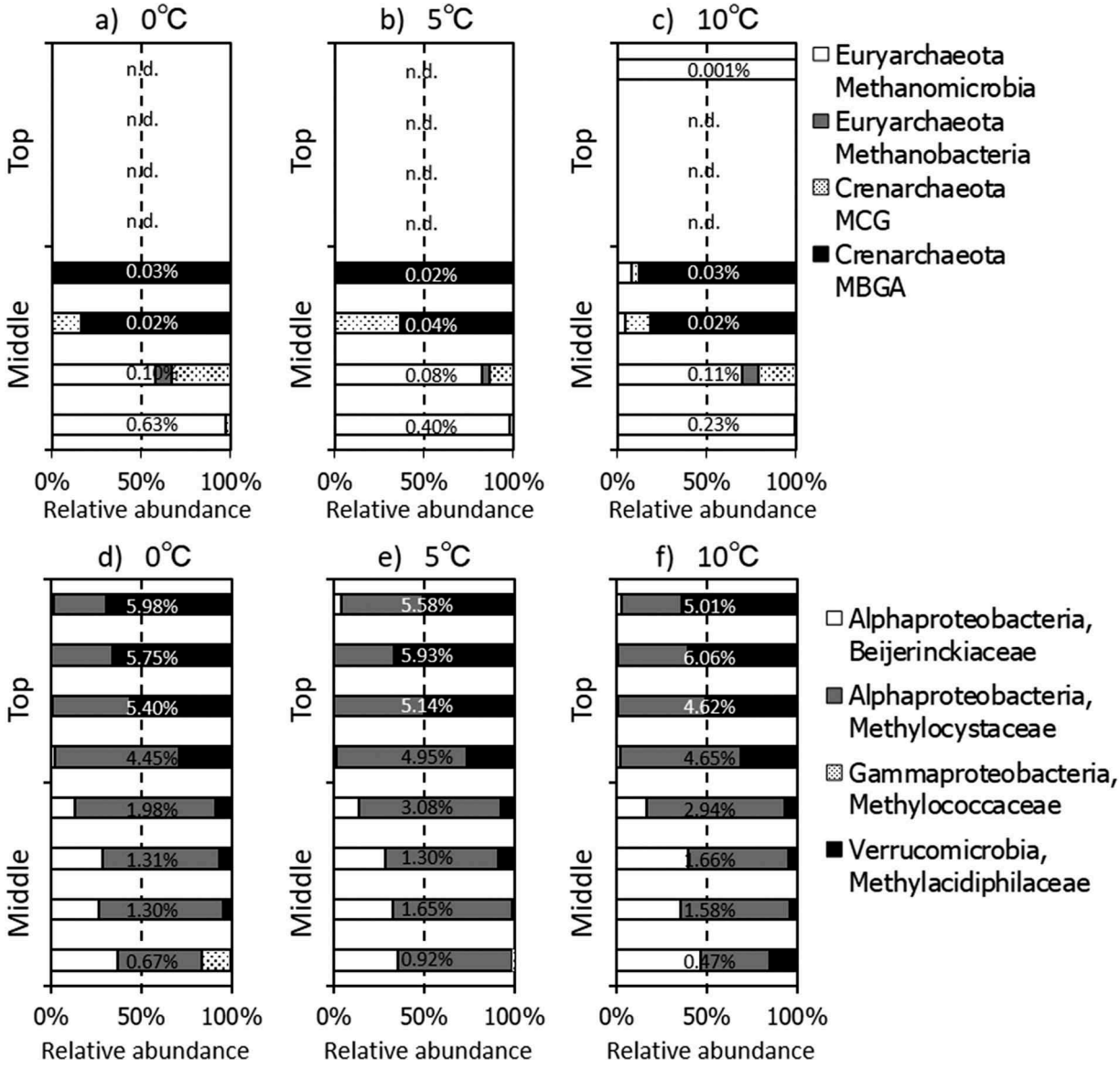

Figure 5. Relative abundances of archaeal classes (a–c) and bacterial methanotroph families (d–f) in soil core samples incubated under weekly changing temperatures from 0°C (a,d) to 5°C (b,e), then 10°C (c,f), without the addition of BES. Both data of archaea and bacterial methanotrophs were extracted from the NGS data shown in Fig. 4. Referring to Semrau *et al*. (2010), relative abundances of OTU categorized to known methanotrophic families of *Methylocystaceae* (a family of α-proteobacteria), *Beijerinckaceae* (a family of α-proteobacteria), *Methylococcaceae* (a family of γ-proteobacteria), and *Methylacidiphilaceae* (a family of Verrucomicrobia) were extracted as relative abundances of bacterial methanotrophs. The values displayed vertically in the centers of the panels are the relative abundances of archaea and bacterial methanotrophs to the overall archaeal and bacterial community (n.d. means not determined).

middle-layer soil samples. *Methanomicrobia* was also detected in the most upper top-layer soil sample incubated at 10°C, but relative abundance to the overall community was only 0.001%. Then, four bacterial communities known as methanotrophs, i.e., *Methylocystaceae* (a family of α-proteobacteria), *Beijerinckiaceae* (a family of α-proteobacteria), *Methylococcaceae* (a family of γ-proteobacteria), and *Methylacidiphilaceae* (a family of Verrucomicrobia) (as shown in Table 4 of Semrau *et al*. 2010), were detected in our samples. Relative abundances of these bacterial methanotrophs to the overall community were 6% in top-layer samples, then reduced to 0.47% in the deepest middle-layer samples. As well as observed in previously described two communities, dominant bacterial methanotrophs also changed from *Methylacidiphilaceae* (a family of Verrucomicrobia) in the most upper top-layer samples, to *Methylocystaceae* (a family of α-proteobacteria) or *Beijerinckiaceae* (a family of α-proteobacteria) in the deepest middle-layer samples.

Then, the NMDS ordination for visualizing similarity of 16S rRNA-based microbial community structures among incubated samples placed same depth samples in similar positions to each other, regardless of temperature differences (Fig. 6). The perMANOVA showed that >80% of variation in bacterial and archaeal community structures among samples were explained by depth of samples. Effects of temperature, then interactions between temperature and depth were negligible ($R^2 \geq 0.05$, $p \geq 0.14$). These patterns of statistical comparisons of bacterial and archaeal community structures were common regardless to the comparison within single layer or through two layers.

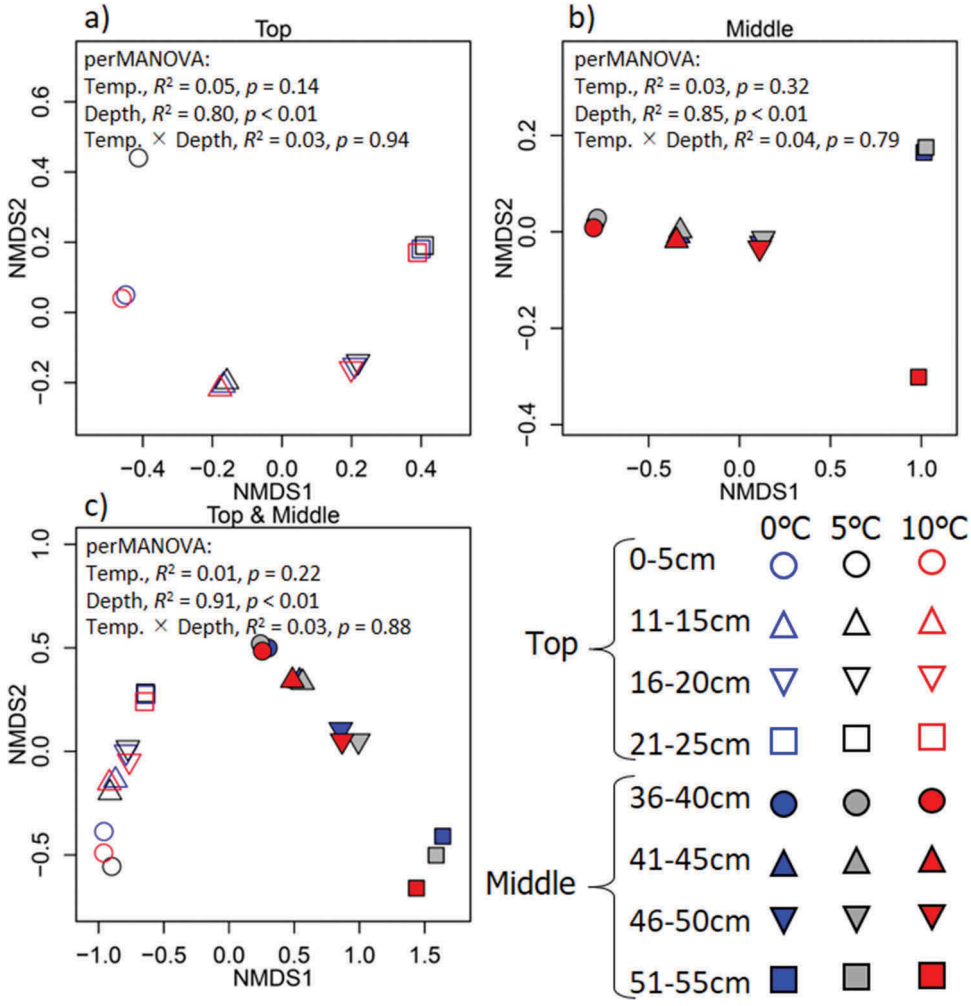

Figure 6. The NMDS ordinations visualizing the pairwise Bray–Curtis dissimilarity matrices for 16S rRNA-based microbial community structures in soil core samples incubated under weekly changing temperatures from 0 to 10°C in intervals of 5°C, without the addition of BES. Significant p levels of effects from temperature (T), soil sample depths (D), and their interaction ($T \times D$) on the microbial community structures were determined by perMANOVA test, then they are presented on top-left sides of panels, with R^2 values representing contributions of factors to variation in microbial community structures among samples.

4. Discussion

Results showed that GHG release/uptake sensitively responded to temperature increase (i.e., thawing progress), then their responses were various among soil sample depths even within single layer, while 16S rRNA-based community structures of bacteria and archaea were changed along with depth but were less changed during the thawing. Then, our finding of various GHG dynamics among different depths within single layer is the major progress from previous studies conducting the thawing experiments of frozen soil cores collected at similar black spruce forests in interior Alaska (Mackelprang *et al*. 2011; Hultman *et al*. 2015). They investigated two soils from an active layer (30–35 cm depth) and a permafrost layer (65–85 cm depth) under continuously unchanged temperatures (5°C in Mackelprang *et al*. 2011; 5 and 22°C in Hultman *et al*. 2015), presenting evidences that carbon and nitrogen cycles during the thaw were different between active layer and permafrost layer. However, the exact interpretation for mechanisms driving GHG dynamics observed in our study has been remained for future works with more measurements of physical, chemical, and biological parameters potentially changeable with the thawing. In the following paragraphs, we discuss several processes likely involving with observed changes in GHG dynamics during the thawing.

The stimulation of CO_2 release during thawing (Fig. 1) was thought to be driven by transitional changes in the environmental and microbial statuses on addition with the fundamental response of microbial activity to temperature (Davidson *et al*. 1998; Kim *et al*. 2012; Sierra *et al*. 2015). For example, CO_2 release from the top-layer soil samples at 0°C was likely associated with the trapping of the CO_2 produced during the frozen season (Oechel *et al*. 1997; Schimel *et al*. 2006; Sullivan *et al*. 2008). Then, the expected enhancement of substrate and water availabilities (Kim *et al*. 2012) could have led to an increase in CO_2 release observed at 5°C, while substrate availability might have been reduced at 10°C, because our incubation experiment was conducted without the addition of any external substrate.

Then, the release of a large amount of CH_4 from deep soils at 0°C without inhibition by BES (Figs. 2 and 3) was consistent with the results obtained by Byun *et al*. (2017), who elucidated the sharply increasing concentration of microbially produced CH_4 in deep frozen soils collected at an adjacent plot in the JICS

supersite. The CH_4 release unsuppressed by BES from the top- and middle-layer soil samples during the incubation at 0°C (Figs. 1B and C and 2A) was consistent with the findings of previous studies (Friborg *et al*. 1997; Kim *et al*. 2007) that upper-layer soil samples can trap CH_4 during the frozen period, as well as CO_2 (Oechel *et al*. 1997; Schimel *et al*. 2006; Sullivan *et al*. 2008) and deep CH_4 (Byun *et al*. 2017). The suppression of CH_4 release and uptake at 5 and 10°C by BES (Fig. 3) implied that the anaerobic microbial processes of CH_4 production (Conrad 2002) and oxidation (Hinrichs and Boetius 2002) occurred during the period. While further evaluations are needed for demonstrating the BES suppression of CH_4 uptake in aerobically incubated top-layer soil samples, Gupta *et al*. (2013) found a widespread distribution of anaerobic CH_4 oxidation across peatland ecosystems. Thus, the changes in net CO_2 and CH_4 release/uptake rate during the thawing progress of a frozen soil core (Figs. 1–3) were likely associated with concurrent changes in multiple physical, chemical, and biological statuses of soils.

The microbial community changing along with the soil depth (Figs. 4–6) was also found by Taş *et al*. (2014), who investigated an upland Alaskan forest located 40 km northeast of our black spruce forest, in addition to the study of Tripathi *et al*. (2018) at the JICS super site. According to Taş *et al*. (2014), the most abundant phyla in the surface-layer soil samples were *Actinobacteria, Verrucomicrobia, Acidobacteria*, and *Proteobacteria*, while high abundances of *Euryarchaeota*, candidate division AD3, and *Chloroflexi* were found in soil samples of the middle and permafrost layers. These similar community structures among current and previous results (Tripathi *et al*. 2018; Taş *et al*. 2014) could support for postulating that similar 16S rRNA-based microbial community might be found even in frozen soil before thawing, while microbial community before thawing was not analyzed in this study.

The unchanged 16S rRNA-based microbial community during thawing progress, as observed in the soil samples used herein, however, still needs to be examined for bottom-layer soil samples containing permafrost. A study by Mackelprang *et al*. (2011) in a forest 100 km northwest from the JICS supersite found that the responses of various microbial gene abundances to thawing were clearer in the permafrost layer than in the active layer. A recently developed analysis technique that couples two or more culture-independent approaches, called multi-omics analysis, is expected to clarify the dynamic interactions between biogeochemical processes and microbial functioning groups in soils (Hultman *et al*. 2015; Mackelprang *et al*. 2011; Taş *et al*. 2014; Zhou *et al*. 2016).

Finally, it should be noticed that the findings that used single core are not sufficient for any comprehensive and generalized understanding on soil GHG dynamics during the thawing on a vegetation scale. Therefore, future freeze–thaw cycle experiments using multiple soil cores with additional works will reveal both generality and specificity of our current findings in the ecosystem.

5. Conclusion

In this study, we found that soil GHG dynamics responded sensitively and variously to thawing of a frozen soil core from a black spruce forest in Interior Alaska, while the there was less change in 16S rRNA-based microbial community structures during the thawing progress. Of these findings, various GHG dynamic among different depths within single layer is the major progress from previous studies conducting the thawing experiments of frozen soil cores collected from similar black spruce forests in interior Alaska (Mackelprang *et al*. 2011; Hultman *et al*. 2015). The changes in net CO_2 and CH_4 release/uptake rates during thawing were likely driven by concurrent changes in multiple physical, chemical, and biological statuses during the transient period. The specific interpretation should be examined in near future with the measurement of physical, chemical, and biological parameters potentially changeable with the thawing.

Acknowledgments

This study received financial supports from following four research funding resources: the JAMSTEC-IARC Collaboration Study (JICS), with funding provided by Japan Agency for Marine-Earth Science and Technology (JAMSTEC) to the International Arctic Research Center (IARC); Japan Society for the Promotion of Science (JSPS) KAKENHI: [16K14869]; National Research Foundation (NRF) of Korea Grand from the Korean Government (Ministry of Science and ICT): [NRF-2016M1A5A1901769], Circum Arctic Permafrost Environment Change Monitoring, Future Prediction, and Development Techniques of Useful Biomaterials (CAPEC Project); KOPRI (Korea Polar Research Institute) basic research project [PE18010]. The authors thank the graduate-students belonging to the Laboratory of Soil Science, Graduate School of Horticulture, Chiba University, for their supports on preliminary experiments and analysis of this study.

Funding

This work was supported by the Japan Agency for Marine-Earth Science and Technology [the JAMSTEC-IARC Collaboration Study (JICS)];Japan Society for the Promotion of Science [KAKENHI 16K14869];Korea Polar Research Institute [KOPRI basic research project PE18010];Ministry of Science and ICT, Korea [NRF-2016M1A5A1901769].

ORCID

Hirohiko Nagano http://orcid.org/0000-0002-3090-7709
Yongwon Kim http://orcid.org/0000-0002-6167-811X

References

Byun E, Yang JW, Kim Y, Ahn J 2017: Trapped greenhouse gases in the permafrost active layer: preliminary results for methane peaks in vertical profiles of frozen Alaskan soil cores. *Permafr. Periglac. Process.* **28**, 477–484. doi:10.1002/ppp.1935

Caporaso JG, Lauber CL, Walters WA *et al*. 2012: Ultra-high-throughput microbial community analysis on the Illumina HiSeq and MiSeq platforms. *ISME J.* **6**, 1621–1624. doi:10.1038/ismej.2012.8

Chen G, Zhu H, Zhang Y 2003: Soil microbial activities and carbon and nitrogen fixation. *Res. Microbiol.* **154**, 393–398. doi:10.1016/S0923-2508(03)00082-2

Conrad R 2002: Control of microbial methane production in wetland rice fields. *Nutr. Cycl. Agroecosystems.* **64**, 59–69. doi:10.1023/A:1021178713988

Davidson EA, Belk E, Boone RD 1998: Soil water content and temperature as independent or confounded factors controlling soil respiration in a temperate mixed hardwood forest. *Glob. Chang. Biol.* **4**, 217–227. doi:10.1046/j.1365-2486.1998.00128.x

DeSantis TZ, Hugenholtz P, Keller K, Brodie EL, Larsen N, Piceno YM, Phan R, Andersen GL 2006: NAST: a multiple sequence alignment server for

comparative analysis of 16S rRNA genes. *Nucleic Acids Res.* **34**, W394-W399. doi:10.1093/nar/gkl244

Friborg T, Christensen TR, Søgaard H 1997: Rapid response of greenhouse gas emission to early spring thaw in a subarctic mire as shown by micrometeorological techniques. *Geophys. Res. Lett.* **24**, 3061–3064. doi:10.1029/97GL03024

Gupta V, Smemo KA, Yavitt JB, Fowle D, Branfireun B, Basiliko N 2013: Stable isotopes reveal widespread anaerobic methane oxidation across latitude and peatland type. *Environ. Sci. Technol.* **47**, 8273–8279. doi:10.1021/es400484t

Hinrichs K-U, Boetius A 2002: The anaerobic oxidation of methane: new insights in microbial ecology and biogeochemistry. *Ocean Margin Syst.* 457–477. doi:10.1007/978-3-662-05127-6_28

Hultman J, Waldrop MP, Mackelprang R *et al.* 2015: Multi-omics of permafrost, active layer and thermokarst bog soil microbiomes. *Nature.* **521**, 208–212. doi:10.1038/nature14238

Ikawa H, Nakai T, Busey RC *et al.* 2015: Understory CO_2, sensible heat, and latent heat fluxes in a black spruce forest in interior Alaska. *Agric. For. Meteorol.* **214–215**, 80–90. doi:10.1016/j.agrformet.2015.08.247

IPCC 2013: The physical science basis. Contribution of Working Group I to the Fifth Assessment Report of the Intergovernmental Panel on Climate Change. The physical science basis. Contribution of Working Group I to the Fifth Assessment Report of the Intergovernmental Panel on Climate Change. Cambridge United Kingdom and New York, NY, USA.

Kim DG, Vargas R, Bond-Lamberty B, Turetsky MR 2012: Effects of soil rewetting and thawing on soil gas fluxes: a review of current literature and suggestions for future research. *Biogeosciences.* **9**, 2459–2483. doi:10.5194/bg-9-2459-2012

Kim Y, Ueyama M, Nakagawa F, Tsunogai U, Harazono Y, Tanaka N 2007: Assessment of winter fluxes of CO2 and CH4 in boreal forest soils of central Alaska estimated by the profile method and the chamber method: a diagnosis of methane emission and implications for the regional carbon budget. *Tellus. Ser. BChem. Phys. Meteorol.* **59**, 223–233. doi:10.1111/j.1600-0889.2006.00233.x

Klindworth A, Pruesse E, Schweer T, Peplies J, Quast C, Horn M, Glöckner FO 2013: Evaluation of general 16S ribosomal RNA gene PCR primers for classical and next-generation sequencing-based diversity studies. *Nucleic Acids Res.* **41**, e1-e1. doi:10.1093/nar/gks808

Kobayashi H, Yunus AP, Nagai S *et al.* 2016: Latitudinal gradient of spruce forest understory and tundra phenology in Alaska as observed from satellite and ground-based data. *Remote Sens. Environ.* **177**, 160–170. doi:10.1016/j.rse.2016.02.020

Li W, Fu L, Niu B, Wu S, Wooley J 2012: Ultrafast clustering algorithms for metagenomic sequence analysis. *Brief. Bioinform.* **13**, 656–668. doi:10.1093/bib/bbs035

Mackelprang R, Waldrop MP, Deangelis KM, David MM, Chavarria KL, Blazewicz SJ, Rubin EM, Jansson JK 2011: Metagenomic analysis of a permafrost microbial community reveals a rapid response to thaw. *Nature.* **480**, 368–371. doi:10.1038/nature10576

Miyazaki S, Saito K, Mori J *et al.* 2015: The GRENE-TEA model intercomparison project (GTMIP): overview and experiment protocol for Stage 1. *Geosci. Model Dev.* **8**, 2841–2856. doi:10.5194/gmd-8-2841-2015

Nagai S, Nakai T, Saitoh TM, Busey RC, Kobayashi H, Suzuki R, Muraoka H, Kim Y 2013: Seasonal changes in camera-based indices from an open canopy black spruce forest in Alaska, and comparison with indices from a closed canopy evergreen coniferous forest in Japan. *Polar Sci.* **7**, 125–135. doi:10.1016/j.polar.2012.12.001

Nagano H, Ikawa H, Nakai T, Matsushima-Yashima M, Kobayashi H, Kim Y, Suzuki R 2018: Extremely dry environment down-regulates nighttime respiration of a black spruce forest in Interior Alaska. *Agric. For. Meteorol.* **249**, 297–309. doi:10.1016/j.agrformet.2017.11.001

Nakai T, Kim Y, Busey RC, Suzuki R, Nagai S, Kobayashi H, Park H, Sugiura K, Ito A 2013: Characteristics of evapotranspiration from a permafrost black spruce forest in interior Alaska. *Polar Sci.* **7**, 136–148. doi:10.1016/j.polar.2013.03.003

Oechel WC, Vourlitis G, Hastings SJ 1997: Cold season CO_2 emission from arctic soils. *Global Biogeochem. Cycles.* **11**, 163–172. doi:10.1029/96GB03035

Oksanen J, Blanchet FG, Friendly M *et al.* 2018: Vegan: community Ecology Package. https://CRAN.R-project.org/package=vegan

R Core Team 2017: R: A Language and Environment for Statistical Computing. Vienna: R Foundation for Statistical Computing.

Schimel JP, Fahnestock J, Michaelson G, Mikan C, Ping C-L, Romanovsky VE, Welker J 2006: Cold-season production of CO_2 in Arctic soils: can laboratory and field estimates be reconciled through a simple modeling approach? Arctic, Antarct. *Alp. Res.* **38**, 249–256. doi:10.1657/1523-0430(2006)38[249:CPOCIA]2.0.CO;2

Semrau JD, DiSpirito AA, Yoon S 2010: Methanotrophs and copper. *FEMS Microbiol. Rev.* **34**, 496–531. doi:10.1111/j.1574-6976.2010.00212.x

Sierra CA, Trumbore SE, Davidson EA, Vicca S, Janssens I 2015: Sensitivity of decomposition rates of soil organic matter with respect to simultaneous changes in temperature and moisture. *J. Adv. Model. Earth Syst.* **7**, 335–356. doi:10.1002/2014MS000358

Sueyoshi T, Saito K, Miyazaki S *et al.* 2015: The GRENE-TEA Model Intercomparison Project (GTMIP) stage 1 forcing dataset. *Earth Syst. Sci. Data Discuss.* **8**, 703–736. doi:10.5194/essdd-8-703-2015

Sugiura K, Suzuki R, Nakai T *et al.* 2011: Supersite as a common platform for multi-observations in Alaska for a collaborative framework between JAMSTEC and IARC. *JAMSTEC Rep. Res. Dev.* **12**, 61–69. doi:10.5918/jamstecr.12.61

Sullivan PF, Welker JM, Arens SJT, Sveinbjörnsson B 2008: Continuous estimates of CO_2 efflux from arctic and boreal soils during the snow-covered season in Alaska. *J. Geophys. Res. Biogeosciences.* **113**. doi:10.1029/2008JG000715

Suzuki R, Kim Y, Kobayashi H, Nagai S, Saito K, Sugiura K, Iwahana G, Busey RC 2015: Supersite for eco-hydrological observations at boreal forest in Poker Flat Research Range, Alaska. *AsiaFlux Newsl.* **38**, 5.

Taş N, Prestat E, McFarland JW, Wickland KP, Knight R, Berhe AA, Jorgenson T, Waldrop MP, Jansson JK 2014: Impact of fire on active layer and permafrost microbial communities and metagenomes in an upland Alaskan boreal forest. *ISME J.* **8**, 1904–1919. doi:10.1038/ismej.2014.36

Tokida T, Mizoguchi M, Miyazaki T, Kagemoto A, Nagata O, Hatano R 2007: Episodic release of methane bubbles from peatland during spring thaw. *Chemosphere.* **70**, 165–171. doi:10.1016/j.chemosphere.2007.06.042

Tripathi BM, Kim M, Kim Y, Byun E, Yang J-W, Ahn J, Lee YK 2018: Variations in bacterial and archaeal communities along depth profiles of Alaskan soil cores. *Sci. Rep.* **8**, 504. doi:10.1038/s41598-017-18777-x

Wang Q, Garrity GM, Tiedje JM, Cole JR 2007: Naïve Bayesian classifier for rapid assignment of rRNA sequences into the new bacterial taxonomy. *Appl. Environ. Microbiol.* **73**, 5261–5267. doi:10.1128/AEM.00062-07

Zhou X, Fornara D, Ikenaga M, Akagi I, Zhang R, Jia Z 2016: The resilience of microbial community under drying and rewetting cycles of three forest soils. *Front. Microbiol.* **7**, 1–12. doi:10.3389/fmicb.2016.01101